

A Simple Recipe for Contrastively Pre-training Video-First Encoders Beyond 16 Frames

Pinelopi Papalampidi* Skanda Koppula* Shreya Pathak*
 Justin Chiu Joe Heyward Viorica Patraucean Jiajun Shen Antoine Miech
 Andrew Zisserman Aida Nematzdeh
 Google DeepMind

{pinelopi, skandak, shreyapa}@google.com

Abstract

Understanding long, real-world videos requires modeling of long-range visual dependencies. To this end, we explore video-first architectures, building on the common paradigm of transferring large-scale, image-text models to video via shallow temporal fusion. However, we expose two limitations to the approach: (1) decreased spatial capabilities, likely due to poor video-language alignment in standard video datasets, and (2) higher memory consumption, bottlenecking the number of frames that can be processed. To mitigate the memory bottleneck, we systematically analyze the memory/accuracy trade-off of various efficient methods: factorized attention, parameter-efficient image-to-video adaptation, input masking, and multi-resolution patchification. Surprisingly, simply masking large portions of the video (up to 75%) during contrastive pre-training proves to be one of the most robust ways to scale encoders to videos up to 4.3 minutes at 1 FPS. Our simple approach for training long video-to-text models, which scales to 1B parameters, does not add new architectural complexity and is able to outperform the popular paradigm of using much larger LLMs as an information aggregator over segment-based information on benchmarks with long-range temporal dependencies (YouCook2, EgoSchema).

1. Introduction

Long-video understanding requires modeling of the temporal dynamics and long-range visual dependencies of real-world scenes [67, 68]. However, capturing long-range visual content is challenging, even when assisted by large language models (LLMs). In this paper, we overcome demonstrate how to extend video encoders to directly process minutes-long visual content using language grounding and

*Equal contribution.

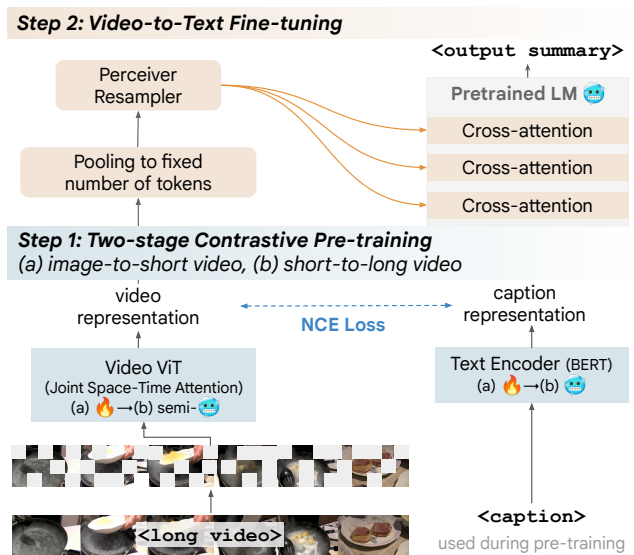


Figure 1. As in Flamingo [1], we first (1) pre-train a visual encoder via Noise Contrastive Estimation, and then (2) use this frozen encoder with a pre-trained LM for video-to-text generation (e.g., video summarization and Q/A). For (1), we propose a two-stage process for pre-training a video encoder: (a) image-to-short video adaptation, and (b) short-to-long video, where we adapt the encoder to longer contexts, using video masking and layer freezing.

overcome hardware memory limitations using simple, established techniques without additional architectural complexity [27, 68]. We focus on long videos through the lens of language, assessing our models on the widely applicable tasks of visual summarization and question-answering.

Recent work on vision-language models have yielded impressive results [1, 33, 76], predominantly focusing on understanding images or short clips of sixteen frames or less [1, 16, 33, 76, 77]. These works recycle strong pre-trained image encoders, and usually perform late temporal fusion [1, 75, 77], and employ mostly-frozen, powerful LLMs. The lack of *video-first* encoders, equipped with

early temporal aggregation, may handicap the ability to process complex visual dependencies, and this is usually reflected in prior work’s focus on short video benchmarks (< 30 seconds) in which sixteen random frames are sufficient for competitive performance [5, 32].

In this work, we follow the standard image–language recipe [1, 33], where we first contrastively pre-train a visual encoder (Step 1; Figure 1) and next plug the frozen pre-trained encoder into a pre-trained LM for tuning video-to-text adapter layers (Step 2; Figure 1). Given this demonstrably scalable and simple-to-tune baseline, we systematically explore *video-first* models. Through our analysis, we are able to scale video-first encoders in a memory-efficient manner to longer sequences of frames, up to 4.3 minutes of video at 1 FPS.

We first explore video-first models on short-video benchmarks (MSR-VTT [71], VATEX [64], YouCook2 [86], ActivityNet [31]) and compare against the SoTA VideoCoCa model [75]. We demonstrate that vanilla joint space-time attention (without factorization) significantly improves performance over frame-level encodings on benchmarks with rich temporal dependencies (YouCook2, VATEX), at the cost of decreased spatial capabilities due to noisy video–text alignments (*e.g.*, objects mentioned in the text but shown in previous or next video segments, text not grounded on visual content) in the pre-training datasets. Overall, our models are able to reach VideoCoCa performance, while requiring fewer parameters and lower frame resolution.

This performance gain incurs extra compute and memory costs that grow quadratically with the video length. To address this, we provide one of the first systematic analyses of the memory/accuracy pareto-front of popular memory-efficient methods; this includes factorized attention, parameter-efficient image-to-video adaptation, input masking, and multi-resolution patchification. Through this analysis, we find that among all these options, simple token masking (up to 75%) during contrastive pre-training incurs only a 1% Recall@1 drop on zero-shot text-video retrieval, and no drop in zero-shot video captioning. At the same time, such high masking offers 2-3x memory savings and allows us to generalize to longer video contexts. The alternatives we explore (*e.g.*, efficient backbone architectures, more sophisticated TubeViT-style patchification [52]), do not maintain the same robustness against noisy video inputs and present a 25% relative decrease in performance for text-video retrieval on challenging benchmarks (YouCook2, VATEX). Finally, although parameter-efficient methods [24, 25] fail to adapt image encoders to video-first models without suffering performance drops, we find that they can adapt video models trained on short contexts (*e.g.*, 16 second videos) to longer temporal horizons.

Based on the above learnings, we extend our best performing short-video encoder to longer contexts of 256

frames (4.3 minutes at 1 FPS). We use the full-length videos of HowTo100M [45] accompanied by LLM-generated summaries based on the ASR to further contrastively train our LONGViViT while masking 75% of the input video tokens and freezing most parameters of the encoder. LONGViViT-to-text (\sim 1B parameters) is able to outperform modular methods that use LLM assistance and PALI-3 [11] for frame captioning on temporally rich benchmarks (YouCook2, EgoSchema). Even modular methods that consider frame selection (SeViLA [78]) or an oracle segmentation of the video for localizing and captioning key events (on YouCook2) cannot reach LONGViViT’s performance. An interesting byproduct of our work is that we can glean which video–language benchmarks have strong temporal dependencies, and thus are suitable for testing long video models; we find that papers often use benchmarks in which short video or even blind models perform well [6, 44, 71].

In short, we provide the following contributions:

- We explore the memory/accuracy pareto-frontier of video-first vision–language models, and systematically evaluate many architectural, data, and training alternatives. In the end, we identify a simple recipe that enables scaling to 4.3 minutes at 1 FPS, many times longer than comparable video–language models [1, 75].
- We identify short and long video benchmarks with substantial temporal dependencies, for which we demonstrate that the traditional image-first, late-temporal fusion recipe is convincingly weaker than a video-first approach.
- Finally, we compare our long video models to a variety of strong baselines and show competitive performance with far fewer parameters; this includes baselines that use LLM-based aggregation over visual captions, and we quantitatively evaluate this common approach for the first time on standard video benchmarks.

2. Related Work

We base our recipes on [1, 33], which provide a strong two-step video–language recipe that leverages the strength of pre-trained LLMs and works at scale. Similar work at smaller scale has additionally included captioning losses [36, 80], more contrastive losses [12, 41, 46, 70], masked autoencoding [18, 19, 22, 38, 43, 58], and combinations thereof [16, 21, 26, 57, 62, 65, 76, 77, 79, 87]. This work largely focuses on image–text modeling and extends to <30 seconds via image-to-video transfer, selective fine-tuning, or temporal fusion of frame encodings [1, 75, 77].

A volume of work focuses on video-first learning. This includes some of the very early work in image-to-video kernel inflation [7, 56, 59], transformer-based video architectures [2, 4, 40], image-to-video parameter-efficient adaptation [8, 39, 49], and multiple spatiotemporal resolutions along different network paths [17, 42, 72, 74]. These have still only been demonstrated on short videos, so other works

have broached the challenge of temporal scalability: [27, 54, 68] propose alternative encoders, and [30, 51, 63] propose more exotic attention mechanisms. TubeViT [52] proposes multi-granularity patchification. We systematically dissect what works and scales among some of these alternatives, electing options that enable us to re-use strong pre-trained models and use standard, more easily-tuned architectures.

Specifically in video-to-text generation, approaches that handle longer videos are very limited and mostly target images or short videos [18, 34, 65]. A dominant approach is to summarize frames and aggregate information via LLMs [34, 37, 66, 81]. To the best of our knowledge, we are the first to attempt to train large-scale video-to-text models on longer sequences of frames and directly test them against LLM-assisted modular methods on challenging temporal benchmarks [44, 86].

3. The Video-to-Text Architecture

We base our approach on the successful two-step recipe that combines pre-trained vision and language models [e.g., 1, 33, 76, 77] as shown in Figure 1: (1) we first follow a two-stage regime for contrastively pre-training the vision encoder, and then (2) fuse the frozen vision representations into a pre-trained, frozen LM.

3.1. Video–Language Contrastive Pre-training

Following common practice [1, 33], we use a dual vision–language architecture with a Noise Contrastive Estimation (NCE) loss [20, 48, 69] to pre-train our vision encoder, similar to CLIP [53], ALIGN [29] and VideoCLIP [70]. Both encoders are transformers [61]: a BERT-medium (77M) or base (117M) language encoder and ViT-Base (86M parameters) or Large (307M parameters) vision encoder. On the language side, caption representations are computed by averaging across the corresponding token representations. On the vision side, video frames are patchified into a sequence of visual tokens, fed into a vision encoder, and then spatiotemporally mean pooled to produce a final video representation.

Most prior larger-scale video–language models use pre-trained image encoders and patchify frames individually via 2D convolutions [e.g., 1, 70, 75]. Instead, we create spatiotemporal tubelets via 3D convolutions as done in recent vision-only models [2, 52, 58]. Using 3D tubelets instead of flat patches has the dual advantage of higher input compression and more explicit temporal contextualization; our early experiments yielded improved performance. The tubelet embedding sequence is then flattened, added to learnable positional embeddings, and fed into the vision encoder. The vision encoder uses spatio-temporal attention as in ViViT [2]: *Joint space-time attention*, which does not add any new parameters to vanilla image ViT [15], facilitating transfer between image and video models. Such seamless

transfer enables us to run a first stage of mixed image and short video pre-training, and a second stage of adapting the encoder to longer videos.

Training a large-scale transformer-based video encoder can be challenging because self-attention across thousands of visual tokens is both compute and memory intensive. Memory bottlenecks a model in two ways: (1) limiting the number of frames, and (2) limiting the contrastive batch size during training, negatively impacting performance. To address (2), we start with an image encoder that is pre-trained with large batch sizes, and further tune it to the video domain, instead of jointly training on images and videos from scratch. For initializing the 3D convolution, we repeat the pre-trained weights across the temporal dimension similarly to [2, 7] (see Appendix A). During video–language pre-training, we maintain different embedding paths for images vs. videos: images are embedded with the original 2D convolution and videos with a separate 3D convolution, with no weight sharing.

3.2. Video-to-Text Tuning

After pre-training the vision encoder, we add a pre-trained LM to generate video descriptions and summaries. We follow previous work [e.g., 1, 76, 77] by keeping the visual encoder frozen and plugging it into a frozen pre-trained LM. We first temporally mean pool the video representations to keep a fixed number of visual tokens independently of the number of frames; interestingly, we find that temporal pooling critically improves training stability for longer videos, while managing to still encode temporal information implicitly in the fixed length tokens (carried over from temporal position embeddings that are added to the video input). We next use a randomly initialized Perceiver resampler [28] to project the representations to the LM embedding space. We add new randomly initialized cross-attention layers at each layer of the LM to ground generation on the visual content. We train these new layers and the Perceiver resampler with a standard auto-regressive video captioning loss: $-\log p(w_t | w < t; \mathcal{V})$, where w_t is its t^{th} token, and \mathcal{V} is the video representation. We provide more details in Appendix A.

4. Memory-Efficient Encoder Design Space

Device memory is a key bottleneck for video training with joint space-time attention. To overcome this, we explore four broad categories of solutions: (1) efficient attention, (2) parameter-efficient image-to-video adaptation, (3) input token masking, and (4) multi-resolution patchification.

1. Attention mechanism. Factorized attention [2, 4] separates the temporal and spatial dimensions over which self-attention is applied, reducing both memory and computational costs. However, this modification introduces a new

temporal block within each transformer layer making initialization and model tuning more challenging. In contrast to [2], that initializes the new blocks with zeroes, we find that we achieve best performance when initializing the temporal blocks with the same self-attention weights of ViT. However, we add a gating mechanism which acts as a residual connection between the self-attention blocks: $h = h + \tanh(\alpha)h_{temporal}$. Here, α is a trainable parameter initialized to zero, that helps maintain the capabilities of the original ViT during training.

2. Parameter-efficient adaptation. We explore using parameter-efficient methods from NLP [9] to adapt image encoders to video, while only tuning a small percentage of model parameters. Most competing approaches adapt image-based models by freezing an image backbone and adding late, trainable temporal-fusion layers [12, 75, 83]. In contrast, we explore ways to use pre-trained image encoders and adapt them to *video-first* architectures [8, 39, 49]. Inspired by the success of parameter-efficient adaptation in NLP [84], we consider using MLP Adapters [24] (after the feedforward block) and LoRA [25] (at the self-attention and feed-forward blocks) at every transformer layer (details in Appendix A). Additionally, we explore tuning only temporal self-attention blocks [8], effectively as adapter layers, in factorized attention. In all variants, we still tune the 3D patch convolution which is new in the video domain.

3. Token masking. Most existing work samples videos at a fixed frames per second (FPS) rate [e.g., 1, 2, 58, 78]. However, semantics required for many video–language tasks vary slowly in the temporal dimension [85] and videos present high degree of redundancy between consecutive frames [21, 58]. We explore ways to sparsely sample the video input to reduce the number of input visual tokens. Specifically, we test random masking of input tubelet embeddings. Since consecutive frames are largely redundant, the same semantic signals could potentially be extracted even with high masking rates. For example, [58] and [21] mask up to 95% of the input video to reach optimal performance on the task of video-masked autoencoding. We demonstrate similar results in a video–language setting.

4. Multi-resolution patchification. Finally, we test a simple approach to reduce redundancy in videos via more coarse-grained patchification in the temporal or spatial dimension, as commonly done in multiple-view video models [17, 42, 74]. However, this decreases frame resolution, and may lose fine-grained information. As a result, we also experiment with TubeViT [52] variant that combines flat patches and tubelets of different granularity to mitigate information loss. Following [52], we use four different con-

volution kernels that can encode either coarse-grained temporal or spatial information; details are in Appendix A.

5. Datasets and Benchmarks

For contrastive pre-training, we use: (1) a set of 27M video-text pairs (VTP) as described in [1], (2) HowTo100M [45] (HT100M; 100M instructional YouTube clips automatically aligned with ASR using their timestamps, called HowTo100M Clips), and (3) VideoCC3M [47] (3M video-text pairs based on Conceptual Captions [55]). Unfortunately, we find the text-video alignment in VideoCC3M to be of poor quality; instead, we use a modified variant where we generate pseudo-labeled captions of every video using PALI [11] (see Appendices B and C). To pre-train with longer videos, we use a long version of HowTo100M (referred to as HowTo100M Summary) consisting of (1) the full-length videos with an average duration of 6.5 minutes and (2) their corresponding textual summaries that we generate by automatically cleaning and summarizing the ASR transcripts using an LLM [23]. We also include the same mixture of image datasets as in [1]. For video-to-text tuning, we use the same mixture of datasets but exclude HowTo100M Clips, since the noisy video-text alignments hurt the performance.

We report text-video retrieval and captioning results on *short video benchmarks*, with average video length ≤ 30 seconds: MSR-VTT [71], YouCook2 [86], ActivityNet Captions [31], and VATEX [64]. To evaluate performance on longer videos, we consider video summarization on full-length versions of YouCook2 and ActivityNet Captions, with a video duration of up to 5 minutes; we also evaluate for multiple-choice video question answering (QA) on EgoSchema [44], a dataset constructed to test long-context temporal understanding.

6. Experimental Results

In Section 6.1, we describe our results evaluating alternatives in memory-efficient video encoder design; options described in Section 4. For this analysis, we use ViT-B/BERT-medium, with training details in Appendix B and ablations on experimental design in Appendix C.

In Section 6.2, we combine our most competitive design choices from 6.1 and test our models on short and long video understanding benchmarks. We scale our best model variants to ViT-L/BERT-base with a 400M (or 1B) language decoder. We test our short video models on text-video retrieval and video captioning, and our long video models on video summarization and QA on 256-frame videos.

In Section 6.3, we share our experience working across short and long video benchmarks [6, 14, 44, 64, 71], offering insights about which ones yield robust temporal signal.

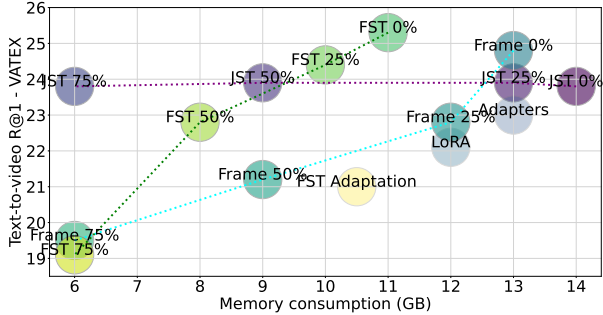
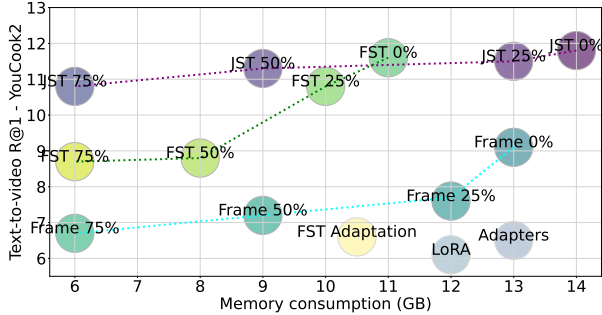


Figure 2. Trade-offs between performance (% text-to-video Recall@1; y axis) and train-time memory consumption (x axis) for different backbones (joint space-time (JST), factorized space-time (FST), and drame-level encodings) with random input masking (0% up to 75%) or parameter-efficient methods for training (Adapters, LoRA, factorized temporal (FST) adaptation; lower opacity).

	MSR-VTT		VATEX		YC2		AN	
	T2V	V2T	T2V	V2T	T2V	V2T	T2V	V2T
Joint ST-ViViT	39.6	38.1	23.8	26.3	12.3	13.6	6.7	6.4
Factorized ST-ViViT	40.2	36.9	25.3	25.4	11.6	12.7	6.6	7.4
Avg Frame-level	39.3	34.8	24.8	25.0	9.1	7.9	6.8	7.1
Att-pool Frame-level	38.4	37.5	21.9	26.1	9.0	8.9	6.1	6.2

Table 1. Text-video retrieval results (% Recall@1) when considering different visual backbones.

6.1. Exploration of Memory-Efficient Designs

We explore memory-efficient methods to train video-first encoders as described in Section 4. We first consider short video inputs of 16 frames at 1 FPS and report peak train-time memory consumption vs. performance on text-video retrieval on short video benchmarks [5]. Then, we test whether our main findings hold for longer inputs (128+ frames) on video summarization on full-length YouCook2.

Base architectures. We explore the memory/accuracy trade-off of different visual backbones in Table 1: ViViT with joint space-time attention (*i.e.*, Joint ST-ViViT), ViViT with factorized attention (*i.e.*, Factorized ST-ViViT) [2], and frame-level (ViT-based) image encodings with average or attentional pooling (‘att-pool’) [1, 75]. Different methods perform similarly, especially on MSR-VTT and ActivityNet (AN). Interestingly, attentional pooling on top of frame-level encodings does not improve performance. ViViT with either joint or factorized attention performs best and presents higher gains for YouCook2 (YC2), the more temporally challenging benchmark [6.3]. In contrast to prior work [*e.g.*, 12, 75] which tests frozen image-to-video transfer and claims joint attention to be inferior, we find it to be competitive in this fully fine-tuned setting.

Architectures and token masking. We now test robustness of backbones when masking part of the input tubelets

(0-75%). We report Recall@1 on text-to-video retrieval for YouCook2 and VATEX¹ per backbone for different masking ratios in Figure 2. Joint space-time attention (JST) is robust against noise from masking up to 75% during pre-training. The same *does not* hold for frame-level encodings and factorized attention (FST), where performance drops consistently as we increase masking. We conclude that JST can better handle noisy inputs and use it in further exploration.

Parameter-efficient adaptation. We next report performance of parameter-efficient image-to-video adaptation in Figure 2. We consider (1) JST with (a) MLP *Adapters* at every layer of the encoder, (b) *LoRA* with rank decomposition matrices in the self-attention and feed-forward transformer blocks, and (2) *factorized temporal adaptation* where we tune the temporal self-attention. No adaptation method can reach the memory savings provided by high input masking, since we tune parameters *depthwise* and gradient computation still requires backpropagation through the model. At the same time, we see significant performance drop, suggesting that adaptation of spatial-only models to the temporal dimension cannot be sufficiently addressed in semi-frozen fashion. Comparing parameter-efficient methods, we find MLP *Adapters* to be more competitive than *LoRA*, which is now canonical for LLMs. We hypothesize that *LoRA* is successful for tuning very small portions of the network and performing “easier” in-modality transfer.

Adaptation at scale. We next scale from ViT-B/86M to ViT-L/307M in Figure 4 and test whether observations hold with different model scales. We present the % memory increase from base to large (left bar set) and % performance *decrease* of each method at each scale². Joint ST exhibits a similar memory increase to frame-level, while leading to

¹We do not observe significant sensitivity to input masking for MSR-VTT and ActivityNet Captions across all configurations (Section 6.3).

²Performance drop for factorized ST is omitted since the variant without masking leads to out of memory issues.

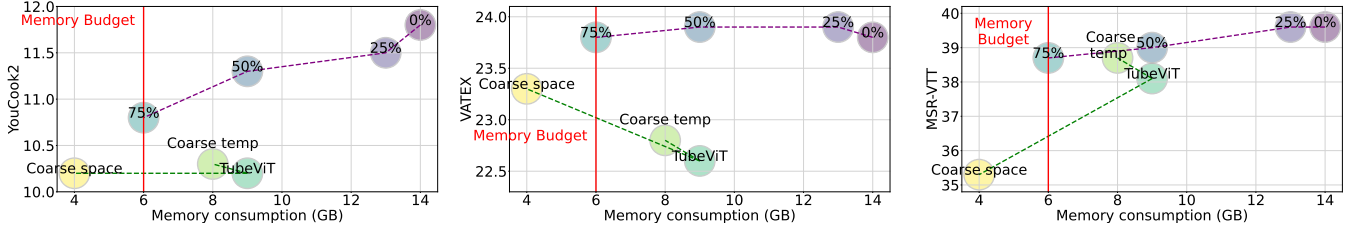


Figure 3. Trade-offs between performance (text-to-video Recall@1; y axis) and memory consumption (x axis) for input sampling methods: (1) high input masking ratios (0% to 75%) with joint space-time attention, (2) coarse-grained temporal (Coarse temp) and/or spatial (Coarse space) patchification with a fixed kernel and TubeViT which samples parts of the video with multiple 3D kernels of different granularity.

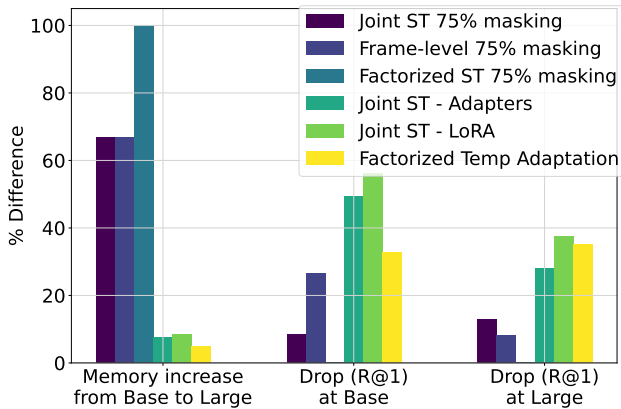


Figure 4. Difference (%) in memory consumption for different model scales: (ViT-B vs ViT-L). We also report performance drop of efficient methods presented in Figure 2 in comparison with the vanilla approach (i.e., no input masking and full fine-tuning) at different model scales to test whether behavior is similar.

smaller accuracy drops, whereas factorized ST presents significant memory overhead with model scale due to the extra temporal self-attention blocks. For this reason, we exclude factorized ST from further experimentation. Finally, parameter-efficient methods are unable to achieve performance similar to their fully fine-tuned counterparts in both model scales, although their memory requirements scale better with model size.

Multi-resolution patchification. Given the outsized memory impact of input token count in Figure 3, we additionally analyze: (1) *coarse-grained patchification* in the temporal (convolution over 4 instead of 2 frames) and/or spatial (convolution over 32x32 instead of 16x16 pixel spaces) dimension, and (2) the *TubeViT* [52] approach of multiple tube kernels of different spatiotemporal size and strides. For all benchmarks, masking the input at high ratios while maintaining a fine granularity of tubelets decreases performance significantly less than other input processing methods. Temporal coarse-grained patchification

negatively affects benchmarks with richer temporal dependencies (i.e., YouCook2, VATEX) more than spatial. The opposite trend holds for datasets depending on spatial understanding (i.e., MSR-VTT, ActivityNet Captions³). TubeViT acts as the middle ground between the two by employing multiple kernels, with some performance degradation across all benchmarks. However, it is not able to alleviate the negative effects caused by considering coarser-grained information and presents higher memory requirements due to the multiple convolutions. Overall, we find that high masking with Joint ST and small tubelets yields the strongest memory/performance curves.

Scaling to longer videos. We now test the best methods from Figure 3 on 128 input frames (32.7k visual tokens). We select methods that are within a memory budget (red vertical lines) and would fit on a 16GB device when expanded to long videos (128+ frames). We contrastively fine-tune [3.1] our best performing video model (i.e., Joint ST referred to as SHORTVIVIT) on sequences of 128 frames on HowTo100M Summary [5], as detailed in Appendix B. We refer to this model as LONGVIVIT. Finally, we fine-tune LONGVIVIT for text generation (Section 3.2) on the full-length YouCook2, and report Rouge-L in Figure 5, measuring memory consumption during both long-context contrastive (*x*-axis) and video-to-text (*y*-axis) tuning.

Validating our previous results, IMAGEViT (frame-level encodings) trained on longer videos with 75% masking⁴ significantly under-performs video-first models (10 R-L drop). SHORTViT without further HT100M Summary training performs better than IMAGEViT, but cannot match models adapted to longer videos. LONGVIVIT improves performance by 1.8 Rouge-L points over SHORTViT. Comparing input masking with coarser-grained patchification⁵ provides similar insights to the previous paragraph.

Finally, we test MLP Adapters [24] for tuning SHORTViT to longer videos and observe no performance drop

³Omitted from Figure 3 but follows same patterns as MSR-VTT.

⁴We start from IMAGEViT trained on short videos with no masking.

⁵Using the same fine-grained SHORTVIVIT model for initialization.

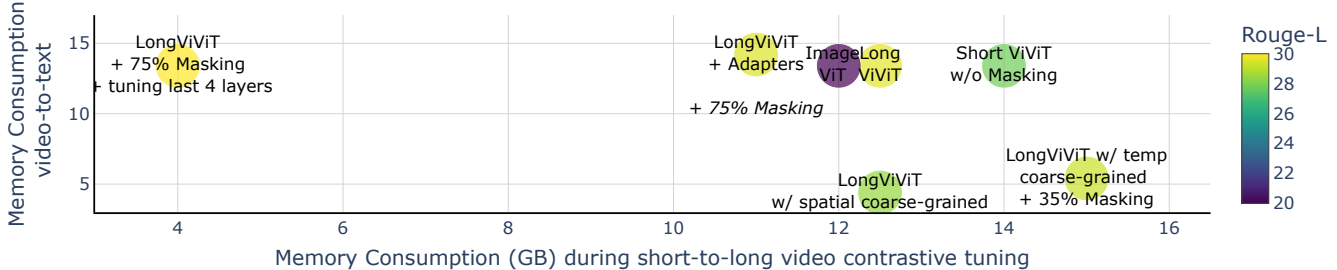


Figure 5. Scaling memory-efficient methods to more frames (i.e., 128 frames) for ViViT-B and variants. We measure performance for video-to-text summarization on the full-length YouCook2 videos via Rouge-L (color-coded) while keeping track of memory consumption during short-to-long video contrastive tuning (x -axis) and video-to-text tuning (y -axis).

	MSR-VTT			VATEX			YouCook2			ActivityNet		
	Zero-shot		FT	Zero-shot		FT	Zero-shot		FT	Zero-shot		FT
	T2V/V2T	C1/C2	C1	T2V/V2T	C1/C2	C1	T2V/V2T	C1/C2	C1	T2V/V2T	C1/C2	C1
IMAGEViT-L	30.9/41.6	24.6/25.1	63.6	36.2/42.9	37.9/39.4	61.1	18.2/16.8	14.5/16.5	95.9	20.6/18.2	16.3/17.7	41.1
SHORTViViT-L	31.9/38.9	32.7/32.9	63.1	37.8/42.8	43.6/43.0	67.5	20.4/20.5	21.0/22.1	131.9	21.3/18.9	25.2/26.1	44.8
EffSHORTViViT-L	29.9/38.3	33.8/33.9	63.8	34.4/42.7	41.3/42.7	64.7	20.5/20.3	21.1/21.7	127.1	20.1/17.7	27.0/26.5	41.1
VideoCoCa-L [75]	33.3 /-	24.3	-	-	-	-	18.9/-	20.7	-	31.5*/-	17.4	-
VideoCoCa-2.1B	<u>34.3/64.7</u>	27.1	<u>73.2</u>	<u>53.2/73.6</u>	22.8	<u>77.8</u>	20.3/-	34.3	128.0	34.5*/33.0*	19.3	39.3
Flamingo-3B [1]	-	-	-	-	40.1	-	-	<u>55.8</u>	-	-	-	-

Table 2. We present three model variants: IMAGEViT-L, that uses frame-level encodings with a late temporal fusion trained on images and videos, SHORTViViT-L, our best performing video-first model with joint space-time attention, and Efficient SHORTViViT-L (EffSHORTViViT-L) where we apply 75% train-time masking for 3x memory savings. We also report performance for SoTA image-first models: VideoCoCa-L and Flamingo-3B, although they are bigger and not directly comparable. We report Recall@1 for zero-shot text-to-video (T2V) and video-to-text (V2T) retrieval, and CIDEr for zero-shot and fine-tuned (FT) captioning when considering a 400M (C1) or 1B (C2) frozen LM for generation. ActivityNet retrieval results marked with * are not directly comparable, as these models uniformly sample frames, whereas we use the first frames of the long video with a fixed FPS of 1 to match experimental settings across benchmarks.

in comparison with full fine-tuning. This provides further evidence that parameter-efficient methods can be used for “easier transfers” but not temporal adaptation of spatial-only models. One downside of MLP Adapters is that it increases parameter count during video-to-text tuning (y -axis in Figure 5). Thus, we also experiment with contrastively tuning only the last four layers of the model. With this, we observe a further 3x decrease in memory, since we tune the network *widthwise* and excise early layer gradient computation. At the same time, there is no memory increase for video-to-text and no performance degradation. We conclude that this combination (high input masking and tuning the last layers) is an effective setting for longer video adaptation. Given the observed robustness to masking, to further decrease video-to-text memory, we also mask 30% of the input video during training and inference without observing any drop in summarization performance (see Appendix C).

6.2. Main Results

Short video benchmarks. We present our main results on short video benchmarks in Table 2. We use ViT-L with BERT-base for contrastive pre-training (Section 3.1) and a

400M frozen LM for video-to-text tuning (Section 3.2). Our entire video-to-text model accounts for $\sim 900\text{M}$ parameters, although we additionally test scaling the frozen LM to 1B parameters ($\sim 1.5\text{B}$ total count). We report Recall@1 for zero-shot text-video retrieval and CIDEr for zero-shot and fine-tuned video captioning. We consider three model variants: frame-level encodings IMAGEViT, SHORTViViT, and SHORTViViT with 75% masking that uses 2-3x less memory (referred to as *Efficient* SHORTViViT). We also report results for VideoCoCa [75] and Flamingo [1]⁶.

Our results remain consistent with our earlier observations. Contextualizing only intra-frame dependencies coupled with late temporal fusion (IMAGEViT) leads to inferior performance for retrieval and captioning on benchmarks with richer temporal dependencies (YouCook2, VATEX) but performs better on retrieval on MSR-VTT which relies on spatial understanding. Video-first architectures further tuned on video datasets (substantially noisier than curated image ones) improve temporal capabilities at the expense

⁶Models are not directly comparable due to different pre-training datasets, model sizes, training regimes, and input resolution. For instance, [75] fully fine-tune the LM and report results for 576×576 frame resolution instead of 256×256 .

of spatial. For Efficient SHORTVIVIT, we find that masking 75% of the input video causes a performance drop: an average of 1% absolute difference on zero-shot retrieval and no significant difference on zero-shot captioning across all benchmarks. The efficient model still performs similarly or better than IMAGEVIT, especially on captioning and temporally rich benchmarks (e.g., YouCook2, VATEX), while consuming significantly less memory. Finally, when scaling the frozen LM component from 400M to 1B (C1→C2) for zero-shot video-to-text generation, we observe moderate improvements across benchmarks and variants.

We compare our results against large image-based models with SoTA performance on video benchmarks (second block of Table 2). Although results are not directly comparable due to different experimental settings, we are competitive and achieve even better results for temporally rich benchmarks (i.e., YouCook2) on text-video retrieval for models of similar parameter count⁷. Moreover, our models significantly outperform VideoCoCa on most video captioning benchmarks even when considering their much larger versions in the zero-shot setting. Finally, when fine-tuning our video-to-text models with the 400M LM, we are again able to match and surpass the performance of the larger VideoCoCa-2.1B in two out of four benchmarks.

Long video understanding. We further tune LONGVIVIT-L on 256-frame HT100M Summary videos and evaluate zero-shot and fine-tuned summarization (YouCook2, ActivityNet) and QA (EgoSchema released subset); this is shown in Table 3. Although we focus on long videos at 1 FPS, we additionally report results on Perception Test [50] in Appendix D, where videos are short but contain rich temporal dependencies and can benefit from higher FPS.

We consider two families of models. 1. Models that take as input 256 frames (first block of Table 3): IMAGEVIT and SHORTVIVIT pre-trained on 16-frame clips, and LONGVIVIT further trained on 256-frame clips. 2. Modular approaches from prior work (second block of Table 3): (a) SeViLA Localizer [78] for localizing important frames in the long video given a textual query which are then fed into SHORTVIVIT for performing the task⁸, and (b) the popular paradigm of captioning video segments or frames and using an LLM to aggregate information and form coherent summaries or answer questions [34, 37, 81]. We try this latter approach with our short video models (IMAGEVIT, SHORTVIVIT), generating captions over 16-second video segments and then feeding the captions to the September

⁷Video-text retrieval results on ActivityNet Captions are not comparable since we are only considering the first 16 seconds of the video, whereas [75] uniformly sample frames from the entire video (~ 180 seconds).

⁸We select 16 frames using the pre-trained localizer provided by [78]. For video summarization, we use synthetic summaries of the video generated by PALI+Bard as the textual query for retrieving frames.

	Zero-shot			Fine-tuned	
	AN	YC2	ES	AN	YC2
Inference with 256 frames					
IMAGEVIT	14.4	4.6	40.8	23.8	29.4
SHORTVIVIT	15.4	7.0	47.9	24.3	29.5
LONGVIVIT	15.2	20.3	56.8	24.0	30.6
Modular approaches with 16-frame video models					
SeViLA-to-SHORTVIVIT	16.2	4.2	49.6	24.4	28.3
IMAGEVIT-to-Bard	18.1	15.8	35.0	22.9	19.1
+ oracle segments	16.3	16.2	–	22.7	22.1
SHORTVIVIT-to-Bard	19.3	18.1	42.0	22.7	20.8
+ oracle segments	18.3	18.2	–	22.7	24.7
PALI [11] 5B-to-Bard	22.0	19.9	44.8	–	–
Blind Bard	–	–	27.0	–	–
SoTA [73]	–	–	–	36.9	34.6

Table 3. Results on long video-to-text benchmarks. We report Rouge-L for zero-shot and fine-tuned video summarization on ActivityNet Captions (AN) and YouCook2 (YC2) and zero-shot accuracy (%) for multiple choice QA on EgoSchema (ES).

2023 release of Bard, a much larger LLM than the ones used in previous results. We caption clips using uniform video segmentation (every 16 seconds) or an oracle segmentation when available (i.e., we consider ground-truth start and end timestamps for different events within ActivityNet and YouCook2 videos). We also test substituting our small video models with PALI-3 (5B parameters) for frame captioning⁹. Finally, we reference the SoTA fine-tuned performance on ActivityNet and YouCook2, when using specialized models with pre-computed features by multiple networks, object detectors, and domain-specific vocabulary [73].

Looking through Table 3, we find that on ActivityNet, which contains less temporal dependencies [6.3], modular approaches via frame selection or LLM-based aggregation of information (second block) perform well. Frame captioning via PALI combined with the power of LLMs is enough for the task in a zero-shot setting. For fine-tuned models, feeding either the long input or selected frames into SHORTVIVIT perform better than utilizing Bard. On ActivityNet, we see no benefit from training further on longer videos.

In contrast, we find that short video and modular models are insufficient for addressing video tasks with longer-range temporal dependencies (YouCook2, EgoSchema). Adapting SHORTVIVIT to longer contexts (LONGVIVIT) significantly improves performance and achieves the best scores across all comparison approaches. Using Bard as an information aggregator over individual clip captions cannot achieve competitive performance, even when considering an oracle video segmentation for YouCook2 (Lines 3 and 5 in the second block of Table 3). Surprisingly, even using a

⁹We consider captions of key frames per 8 seconds of video.

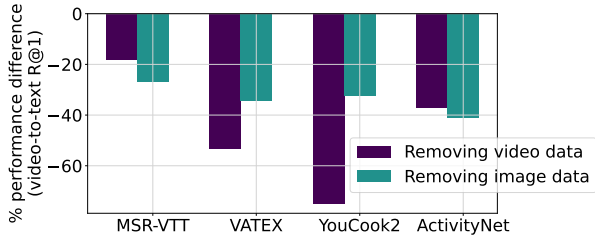


Figure 6. Performance difference (%) per benchmark when we remove (1) video or (2) image data from the training mixture.

much larger and more powerful image-based model (PALI) cannot reach LONGVIVIT on YouCook2 and EgoSchema. Interestingly, selecting 16 key frames and feeding them into SHORTVIVIT also outperforms Bard-based methods on EgoSchema and fine-tuned YouCook2. This suggests there can be temporal dependencies in long videos that cannot be resolved even with an optimal event segmentation for the video, or be aggregated by LLMs given imprecise visual information. On such benchmarks, LONGVIVIT demonstrates strong performance even without LLM assistance.

6.3. Brief Notes on Video Evaluations

We briefly describe some of our findings on video evaluations. Firstly, we find that blind Bard is able to achieve SoTA results on the *full set* of EgoSchema (no visual input; 33.9% accuracy vs. 32.1% for the best model in [44]). Adding visual information from PALI into Bard increases performance to just 39.2%. However, on EgoSchema’s released *subset*, performance of blind Bard is 27%, which is much lower than PALI-to-Bard (44.8%), suggesting that the subset contains questions that rely more on visual grounding than pure language reasoning, so we report numbers on the subset in Table 3 and on the full set in Appendix D.

Figure 6 details a simple ablation across other video benchmarks to quantify temporal richness. We test removing either video or image data from the training mix and measure the effect on performance (video-to-text Recall@1). We see a dramatic performance drop when removing video data for YouCook2 and VATEX (up to 75%). ActivityNet and MSR-VTT suffer more from the absence of image data, whereas non-video training influences performance in lesser degree (as little as 18% for MSR-VTT). We believe there’s room for more fine-grained, temporal-focused video–language benchmarks in the community.

7. Conclusions

In short, we systematically analyze memory-efficient methods to scale video-first architectures to longer sequences of frames and demonstrate that just masking high percentages of the video ($\leq 75\%$) yields competitive results on long video–language tasks. Such masking shows a very small

performance drop on short videos, provides 2-3x memory savings and allows scaling up to 4.3 minutes at 1 FPS (LONGVIVIT) when freezing part of the short video network in our two-stage training. LONGVIVIT outperforms modular approaches with LLM assistance on video summarization and QA on benchmarks with richer temporal dependencies (YouCook2, EgoSchema). We overall demonstrate that encoding longer-range visual dependencies can make a difference in downstream performance and corrects mistakes that LLMs are unable to rectify.

Acknowledgements

We thank Chuhan Zhang for her thoughtful feedback on early drafts of the work; Chris Dyer, Joao Carreira, and Gabriel Brostow for their support, feedback, and guidance through the project; and Lucia Lopez for her valuable help in generating synthetic video captions.

References

- [1] Jean-Baptiste Alayrac, Jeff Donahue, Pauline Luc, Antoine Miech, Iain Barr, Yana Hasson, Karel Lenc, Arthur Mensch, Katherine Millican, Malcolm Reynolds, et al. Flamingo: a visual language model for few-shot learning. *Advances in Neural Information Processing Systems*, 35:23716–23736, 2022. [1](#), [2](#), [3](#), [4](#), [5](#), [7](#), [14](#), [16](#), [17](#), [19](#)
- [2] Anurag Arnab, Mostafa Dehghani, Georg Heigold, Chen Sun, Mario Lučić, and Cordelia Schmid. Vivit: A video vision transformer. In *Proceedings of the IEEE/CVF international conference on computer vision*, pages 6836–6846, 2021. [2](#), [3](#), [4](#), [5](#), [14](#), [17](#)
- [3] Gedas Bertasius, Heng Wang, and Lorenzo Torresani. Is space-time attention all you need for video understanding? In *ICML*, page 4, 2021. [17](#)
- [4] Gedas Bertasius, Heng Wang, and Lorenzo Torresani. Is space-time attention all you need for video understanding? In *ICML*, page 4, 2021. [2](#), [3](#)
- [5] Shyamal Buch, Cristóbal Eyzaguirre, Adrien Gaidon, Jiajun Wu, Li Fei-Fei, and Juan Carlos Niebles. Revisiting the” video” in video-language understanding. In *Proceedings of the IEEE/CVF conference on computer vision and pattern recognition*, pages 2917–2927, 2022. [2](#)
- [6] Fabian Caba Heilbron, Victor Escorcia, Bernard Ghanem, and Juan Carlos Niebles. Activitynet: A large-scale video benchmark for human activity understanding. In *Proceedings of the IEEE conference on computer vision and pattern recognition*, pages 961–970, 2015. [2](#), [4](#)
- [7] Joao Carreira and Andrew Zisserman. Quo vadis, action recognition? a new model and the kinetics dataset. In *Proceedings of the IEEE Conference on Computer Vision and Pattern Recognition*, pages 6299–6308, 2017. [2](#), [3](#), [14](#)
- [8] Dongsheng Chen, Chaofan Tao, Lu Hou, Lifeng Shang, Xin Jiang, and Qun Liu. Litevl: Efficient video-language learning with enhanced spatial-temporal modeling. In *Proceedings of the 2022 Conference on Empirical Methods in Natural Language Processing*, pages 7985–7997, 2022. [2](#), [4](#)
- [9] Jiaao Chen, Aston Zhang, Xingjian Shi, Mu Li, Alex Smola, and Diyi Yang. Parameter-efficient fine-tuning design spaces. *arXiv preprint arXiv:2301.01821*, 2023. [4](#)
- [10] Xinlei Chen, Hao Fang, Tsung-Yi Lin, Ramakrishna Vedantam, Saurabh Gupta, Piotr Dollár, and C Lawrence Zitnick. Microsoft coco captions: Data collection and evaluation server. *arXiv preprint arXiv:1504.00325*, 2015. [17](#)
- [11] Xi Chen, Xiao Wang, Lucas Beyer, Alexander Kolesnikov, Jialin Wu, Paul Voigtlaender, Basil Mustafa, Sebastian Goodman, Ibrahim Alabdulmohsin, Piotr Padlewski, et al. Pali-3 vision language models: Smaller, faster, stronger. *arXiv preprint arXiv:2310.09199*, 2023. [2](#), [4](#), [8](#), [15](#), [19](#)
- [12] Feng Cheng, Xizi Wang, Jie Lei, David Crandall, Mohit Bansal, and Gedas Bertasius. Vindlu: A recipe for effective video-and-language pretraining. In *Proceedings of the IEEE/CVF Conference on Computer Vision and Pattern Recognition*, pages 10739–10750, 2023. [2](#), [4](#), [5](#)
- [13] R Christoph and Feichtenhofer Axel Pinz. Spatiotemporal residual networks for video action recognition. *Advances in neural information processing systems*, 2, 2016. [14](#)
- [14] Pradipto Das, Chenliang Xu, Richard F Doell, and Jason J Corso. A thousand frames in just a few words: Lingual description of videos through latent topics and sparse object stitching. In *Proceedings of the IEEE conference on computer vision and pattern recognition*, pages 2634–2641, 2013. [4](#)
- [15] Alexey Dosovitskiy, Lucas Beyer, Alexander Kolesnikov, Dirk Weissenborn, Xiaohua Zhai, Thomas Unterthiner, Mostafa Dehghani, Matthias Minderer, Georg Heigold, Sylvain Gelly, et al. An image is worth 16x16 words: Transformers for image recognition at scale. In *International Conference on Learning Representations*, 2020. [3](#)
- [16] Danny Driess, Fei Xia, Mehdi SM Sajjadi, Corey Lynch, Aakanksha Chowdhery, Brian Ichter, Ayzaan Wahid, Jonathan Tompson, Quan Vuong, Tianhe Yu, et al. Palm-e: An embodied multimodal language model. *arXiv preprint arXiv:2303.03378*, 2023. [1](#), [2](#)
- [17] Christoph Feichtenhofer, Haoqi Fan, Jitendra Malik, and Kaiming He. Slowfast networks for video recognition. In *Proceedings of the IEEE/CVF international conference on computer vision*, pages 6202–6211, 2019. [2](#), [4](#)
- [18] Tsu-Jui Fu, Linjie Li, Zhe Gan, Kevin Lin, William Yang Wang, Lijuan Wang, and Zicheng Liu. Violet: End-to-end video-language transformers with masked visual-token modeling. *arXiv preprint arXiv:2111.12681*, 2021. [2](#), [3](#), [17](#), [18](#)
- [19] Tsu-Jui Fu, Linjie Li, Zhe Gan, Kevin Lin, William Yang Wang, Lijuan Wang, and Zicheng Liu. An empirical study of end-to-end video-language transformers with masked visual modeling. In *Proceedings of the IEEE/CVF Conference on Computer Vision and Pattern Recognition*, pages 22898–22909, 2023. [2](#)
- [20] Michael Gutmann and Aapo Hyvärinen. Noise-contrastive estimation: A new estimation principle for unnormalized statistical models. In *Proceedings of the thirteenth international conference on artificial intelligence and statistics*, pages 297–304. JMLR Workshop and Conference Proceedings, 2010. [3](#)
- [21] Tengda Han, Weidi Xie, and Andrew Zisserman. Turbo training with token dropout. *arXiv preprint arXiv:2210.04889*, 2022. [2](#), [4](#)
- [22] Kaiming He, Xinlei Chen, Saining Xie, Yanghao Li, Piotr Dollár, and Ross B Girshick. Masked autoencoders are scalable vision learners. 2022 IEEE. In *CVF Conference on Computer Vision and Pattern Recognition (CVPR)*, pages 15979–15988, 2021. [2](#)
- [23] Jordan Hoffmann, Sebastian Borgeaud, Arthur Mensch, Elena Buchatskaya, Trevor Cai, Eliza Rutherford, Diego de Las Casas, Lisa Anne Hendricks, Johannes Welbl, Aidan Clark, et al. Training compute-optimal large language models. *arXiv preprint arXiv:2203.15556*, 2022. [4](#), [15](#)
- [24] Neil Houlsby, Andrei Giurgiu, Stanislaw Jastrzebski, Bruna Morrone, Quentin De Laroussilhe, Andrea Gesmundo, Mona Attariyan, and Sylvain Gelly. Parameter-efficient transfer learning for nlp. In *International Conference on Machine Learning*, pages 2790–2799. PMLR, 2019. [2](#), [4](#), [6](#), [14](#)
- [25] Edward J Hu, Phillip Wallis, Zeyuan Allen-Zhu, Yuanzhi Li, Shean Wang, Lu Wang, Weizhu Chen, et al. Lora: Low-

- rank adaptation of large language models. In *International Conference on Learning Representations*, 2021. 2, 4, 14
- [26] Shaohan Huang, Li Dong, Wenhui Wang, Yaru Hao, Saksham Singhal, Shuming Ma, Tengchao Lv, Lei Cui, Owais Khan Mohammed, Qiang Liu, et al. Language is not all you need: Aligning perception with language models. *arXiv preprint arXiv:2302.14045*, 2023. 2
- [27] Md Mohaiminul Islam and Gedas Bertasius. Long movie clip classification with state-space video models. In *European Conference on Computer Vision*, pages 87–104. Springer, 2022. 1, 3
- [28] Andrew Jaegle, Felix Gimeno, Andy Brock, Oriol Vinyals, Andrew Zisserman, and Joao Carreira. Perceiver: General perception with iterative attention. In *International conference on machine learning*, pages 4651–4664. PMLR, 2021. 3
- [29] Chao Jia, Yinfei Yang, Ye Xia, Yi-Ting Chen, Zarana Parekh, Hieu Pham, Quoc Le, Yun-Hsuan Sung, Zhen Li, and Tom Duerig. Scaling up visual and vision-language representation learning with noisy text supervision. In *International Conference on Machine Learning*, pages 4904–4916. PMLR, 2021. 3, 16, 17
- [30] Nikita Kitaev, Łukasz Kaiser, and Anselm Levskaya. Reformer: The efficient transformer. *arXiv preprint arXiv:2001.04451*, 2020. 3
- [31] Ranjay Krishna, Kenji Hata, Frederic Ren, Li Fei-Fei, and Juan Carlos Niebles. Dense-captioning events in videos. In *Proceedings of the IEEE international conference on computer vision*, pages 706–715, 2017. 2, 4
- [32] Jie Lei, Tamara L Berg, and Mohit Bansal. Revealing single frame bias for video-and-language learning. *arXiv preprint arXiv:2206.03428*, 2022. 2
- [33] Junnan Li, Dongxu Li, Silvio Savarese, and Steven Hoi. Blip-2: Bootstrapping language-image pre-training with frozen image encoders and large language models. *arXiv preprint arXiv:2301.12597*, 2023. 1, 2, 3
- [34] KunChang Li, Yinan He, Yi Wang, Yizhuo Li, Wenhui Wang, Ping Luo, Yali Wang, Limin Wang, and Yu Qiao. Videochat: Chat-centric video understanding. *arXiv preprint arXiv:2305.06355*, 2023. 3, 8
- [35] Linjie Li, Zhe Gan, Kevin Lin, Chung-Ching Lin, Zicheng Liu, Ce Liu, and Lijuan Wang. Lavender: Unifying video-language understanding as masked language modeling. *arXiv preprint arXiv:2206.07160*, 2022. 17, 18
- [36] Linjie Li, Zhe Gan, Kevin Lin, Chung-Ching Lin, Zicheng Liu, Ce Liu, and Lijuan Wang. Lavender: Unifying video-language understanding as masked language modeling. In *Proceedings of the IEEE/CVF Conference on Computer Vision and Pattern Recognition*, pages 23119–23129, 2023. 2
- [37] Kevin Lin, Faisal Ahmed, Linjie Li, Chung-Ching Lin, Ehsan Azarnasab, Zhengyuan Yang, Jianfeng Wang, Lin Liang, Zicheng Liu, Yumao Lu, Ce Liu, and Lijuan Wang. Mm-vid: Advancing video understanding with gpt-4v(ision), 2023. 3, 8
- [38] Yuanze Lin, Chen Wei, Huiyu Wang, Alan Yuille, and Cihang Xie. Smaug: Sparse masked autoencoder for efficient video-language pre-training. In *Proceedings of the IEEE/CVF International Conference on Computer Vision*, pages 2459–2469, 2023. 2
- [39] Ruyang Liu, Jingjia Huang, Ge Li, Jiashi Feng, Xinglong Wu, and Thomas H Li. Revisiting temporal modeling for clip-based image-to-video knowledge transferring. In *Proceedings of the IEEE/CVF Conference on Computer Vision and Pattern Recognition*, pages 6555–6564, 2023. 2, 4
- [40] Ze Liu, Jia Ning, Yue Cao, Yixuan Wei, Zheng Zhang, Stephen Lin, and Han Hu. Video swin transformer. In *Proceedings of the IEEE/CVF conference on computer vision and pattern recognition*, pages 3202–3211, 2022. 2
- [41] Huaishao Luo, Lei Ji, Ming Zhong, Yang Chen, Wen Lei, Nan Duan, and Tianrui Li. Clip4clip: An empirical study of clip for end to end video clip retrieval and captioning. *Neurocomputing*, 508:293–304, 2022. 2, 17
- [42] Chuofan Ma, Qiushan Guo, Yi Jiang, Ping Luo, Zehuan Yuan, and Xiaojuan Qi. Rethinking resolution in the context of efficient video recognition. *Advances in Neural Information Processing Systems*, 35:37865–37877, 2022. 2, 4
- [43] Yue Ma, Tianyu Yang, Yin Shan, and Xiu Li. Simvtp: Simple video text pre-training with masked autoencoders. *arXiv preprint arXiv:2212.03490*, 2022. 2
- [44] Karttikeya Mangalam, Raiymbek Akshulakov, and Jitendra Malik. Egoschema: A diagnostic benchmark for very long-form video language understanding. *arXiv preprint arXiv:2308.09126*, 2023. 2, 3, 4, 9, 16, 19
- [45] Antoine Miech, Dimitri Zhukov, Jean-Baptiste Alayrac, Makarand Tapaswi, Ivan Laptev, and Josef Sivic. Howto100m: Learning a text-video embedding by watching hundred million narrated video clips. In *Proceedings of the IEEE/CVF International Conference on Computer Vision*, pages 2630–2640, 2019. 2, 4, 16
- [46] Antoine Miech, Jean-Baptiste Alayrac, Lucas Smaira, Ivan Laptev, Josef Sivic, and Andrew Zisserman. End-to-end learning of visual representations from uncurated instructional videos. In *Proceedings of the IEEE/CVF Conference on Computer Vision and Pattern Recognition*, pages 9879–9889, 2020. 2, 17
- [47] Arsha Nagrani, Paul Hongsuck Seo, Bryan Seybold, Anja Hauth, Santiago Manen, Chen Sun, and Cordelia Schmid. Learning audio-video modalities from image captions. In *Computer Vision—ECCV 2022: 17th European Conference, Tel Aviv, Israel, October 23–27, 2022, Proceedings, Part XIV*, pages 407–426. Springer, 2022. 4, 16
- [48] Aaron van den Oord, Yazhe Li, and Oriol Vinyals. Representation learning with contrastive predictive coding. *arXiv preprint arXiv:1807.03748*, 2018. 3
- [49] Junting Pan, Ziyi Lin, Xiatian Zhu, Jing Shao, and Hongsheng Li. St-adapter: Parameter-efficient image-to-video transfer learning. *Advances in Neural Information Processing Systems*, 35:26462–26477, 2022. 2, 4
- [50] Viorica Pătrăucean, Lucas Smaira, Ankush Gupta, Adrià Recasens Contente, Larisa Markeeva, Dylan Banarse, Skanda Koppula, Joseph Heyward, Mateusz Malinowski, Yi Yang, et al. Perception test: A diagnostic benchmark for multimodal video models. *arXiv preprint arXiv:2305.13786*, 2023. 8, 19

- [51] Bowen Peng, Jeffrey Quesnelle, Honglu Fan, and Enrico Shippole. Yarn: Efficient context window extension of large language models. *arXiv preprint arXiv:2309.00071*, 2023. [3](#)
- [52] AJ Piergiovanni, Weicheng Kuo, and Anelia Angelova. Rethinking video vits: Sparse video tubes for joint image and video learning. In *Proceedings of the IEEE/CVF Conference on Computer Vision and Pattern Recognition*, pages 2214–2224, 2023. [2](#), [3](#), [4](#), [6](#), [14](#)
- [53] Alec Radford, Jong Wook Kim, Chris Hallacy, Aditya Ramesh, Gabriel Goh, Sandhini Agarwal, Girish Sastry, Amanda Askell, Pamela Mishkin, Jack Clark, et al. Learning transferable visual models from natural language supervision. In *International conference on machine learning*, pages 8748–8763. PMLR, 2021. [3](#), [17](#)
- [54] Michael S Ryoo, Keerthana Gopalakrishnan, Kumara Kahatapitiya, Ted Xiao, Kanishka Rao, Austin Stone, Yao Lu, Julian Ibarz, and Anurag Arnab. Token turing machines. In *Proceedings of the IEEE/CVF Conference on Computer Vision and Pattern Recognition*, pages 19070–19081, 2023. [3](#)
- [55] Piyush Sharma, Nan Ding, Sebastian Goodman, and Radu Soricut. Conceptual captions: A cleaned, hypernymed, image alt-text dataset for automatic image captioning. In *Proceedings of the 56th Annual Meeting of the Association for Computational Linguistics (Volume 1: Long Papers)*, pages 2556–2565, 2018. [4](#)
- [56] Karen Simonyan and Andrew Zisserman. Two-stream convolutional networks for action recognition in videos. *Advances in neural information processing systems*, 27, 2014. [2](#)
- [57] Amanpreet Singh, Ronghang Hu, Vedanuj Goswami, Guillaume Couairon, Wojciech Galuba, Marcus Rohrbach, and Douwe Kiela. Flava: A foundational language and vision alignment model. In *Proceedings of the IEEE/CVF Conference on Computer Vision and Pattern Recognition*, pages 15638–15650, 2022. [2](#)
- [58] Zhan Tong, Yibing Song, Jue Wang, and Limin Wang. Videomae: Masked autoencoders are data-efficient learners for self-supervised video pre-training. In *Advances in Neural Information Processing Systems*, 2022. [2](#), [3](#), [4](#)
- [59] Du Tran, Heng Wang, Lorenzo Torresani, Jamie Ray, Yann LeCun, and Manohar Paluri. A closer look at spatiotemporal convolutions for action recognition. In *Proceedings of the IEEE conference on Computer Vision and Pattern Recognition*, pages 6450–6459, 2018. [2](#)
- [60] Michael Tschannen, Manoj Kumar, Andreas Steiner, Xiaohua Zhai, Neil Houlsby, and Lucas Beyer. Image captioners are scalable vision learners too. *arXiv preprint arXiv:2306.07915*, 2023. [17](#)
- [61] Ashish Vaswani, Noam Shazeer, Niki Parmar, Jakob Uszkoreit, Llion Jones, Aidan N Gomez, Łukasz Kaiser, and Illia Polosukhin. Attention is all you need. *Advances in neural information processing systems*, 30, 2017. [3](#)
- [62] Junke Wang, Dongdong Chen, Zuxuan Wu, Chong Luo, Luwei Zhou, Yucheng Zhao, Yujia Xie, Ce Liu, Yu-Gang Jiang, and Lu Yuan. Omnivl: One foundation model for image-language and video-language tasks. *Advances in neural information processing systems*, 35:5696–5710, 2022. [2](#)
- [63] Sinong Wang, Belinda Z Li, Madian Khabsa, Han Fang, and Hao Ma. Linformer: Self-attention with linear complexity. *arXiv preprint arXiv:2006.04768*, 2020. [3](#)
- [64] Xin Wang, Jiawei Wu, Junkun Chen, Lei Li, Yuan-Fang Wang, and William Yang Wang. Vatex: A large-scale, high-quality multilingual dataset for video-and-language research. In *Proceedings of the IEEE/CVF International Conference on Computer Vision*, pages 4581–4591, 2019. [2](#), [4](#)
- [65] Yi Wang, Kunchang Li, Yizhuo Li, Yinan He, Bingkun Huang, Zhiyu Zhao, Hongjie Zhang, Jilan Xu, Yi Liu, Zun Wang, et al. Internvideo: General video foundation models via generative and discriminative learning. *arXiv preprint arXiv:2212.03191*, 2022. [2](#), [3](#), [16](#), [19](#)
- [66] Zhenhailong Wang, Manling Li, Ruochen Xu, Luwei Zhou, Jie Lei, Xudong Lin, Shuohang Wang, Ziyi Yang, Chenguang Zhu, Derek Hoiem, et al. Language models with image descriptors are strong few-shot video-language learners. *Advances in Neural Information Processing Systems*, 35: 8483–8497, 2022. [3](#)
- [67] Chao-Yuan Wu and Philipp Krahenbuhl. Towards long-form video understanding. In *Proceedings of the IEEE/CVF Conference on Computer Vision and Pattern Recognition*, pages 1884–1894, 2021. [1](#)
- [68] Chao-Yuan Wu, Yanghao Li, Kartikeya Mangalam, Haoqi Fan, Bo Xiong, Jitendra Malik, and Christoph Feichtenhofer. Memvit: Memory-augmented multiscale vision transformer for efficient long-term video recognition. In *Proceedings of the IEEE/CVF Conference on Computer Vision and Pattern Recognition*, pages 13587–13597, 2022. [1](#), [3](#)
- [69] Zhirong Wu, Yuanjun Xiong, Stella X Yu, and Dahua Lin. Unsupervised feature learning via non-parametric instance discrimination. In *Proceedings of the IEEE conference on computer vision and pattern recognition*, pages 3733–3742, 2018. [3](#)
- [70] Hu Xu, Gargi Ghosh, Po-Yao Huang, Dmytro Okhonko, Armen Aghajanyan, Florian Metze, Luke Zettlemoyer, and Christoph Feichtenhofer. Videoclip: Contrastive pre-training for zero-shot video-text understanding. In *Proceedings of the 2021 Conference on Empirical Methods in Natural Language Processing*, pages 6787–6800, 2021. [2](#), [3](#), [17](#)
- [71] Jun Xu, Tao Mei, Ting Yao, and Yong Rui. Msr-vtt: A large video description dataset for bridging video and language. In *Proceedings of the IEEE conference on computer vision and pattern recognition*, pages 5288–5296, 2016. [2](#), [4](#)
- [72] Hongwei Xue, Tiankai Hang, Yanhong Zeng, Yuchong Sun, Bei Liu, Huan Yang, Jianlong Fu, and Baining Guo. Advancing high-resolution video-language representation with large-scale video transcriptions. In *Proceedings of the IEEE/CVF Conference on Computer Vision and Pattern Recognition*, pages 5036–5045, 2022. [2](#)
- [73] Kashu Yamazaki, Khoa Vo, Quang Sang Truong, Bhiksha Raj, and Ngan Le. Vltint: visual-linguistic transformer-in-transformer for coherent video paragraph captioning. In *Proceedings of the AAAI Conference on Artificial Intelligence*, pages 3081–3090, 2023. [8](#)
- [74] Shen Yan, Xuehan Xiong, Anurag Arnab, Zhichao Lu, Mi Zhang, Chen Sun, and Cordelia Schmid. Multiview

- transformers for video recognition. In *Proceedings of the IEEE/CVF conference on computer vision and pattern recognition*, pages 3333–3343, 2022. [2](#), [4](#), [17](#)
- [75] Shen Yan, Tao Zhu, Zirui Wang, Yuan Cao, Mi Zhang, Soham Ghosh, Yonghui Wu, and Jiahui Yu. Video-text modeling with zero-shot transfer from contrastive captioners. *arXiv preprint arXiv:2212.04979*, 2022. [1](#), [2](#), [3](#), [4](#), [5](#), [7](#), [8](#), [15](#), [17](#), [18](#)
- [76] Antoine Yang, Antoine Miech, Josef Sivic, Ivan Laptev, and Cordelia Schmid. Zero-shot video question answering via frozen bidirectional language models. *Advances in Neural Information Processing Systems*, 35:124–141, 2022. [1](#), [2](#), [3](#)
- [77] Qinghao Ye, Haiyang Xu, Guohai Xu, Jiabo Ye, Ming Yan, Yiyang Zhou, Junyang Wang, Anwen Hu, Pengcheng Shi, Yaya Shi, et al. mplug-owl: Modularization empowers large language models with multimodality. *arXiv preprint arXiv:2304.14178*, 2023. [1](#), [2](#), [3](#)
- [78] Shoubin Yu, Jaemin Cho, Prateek Yadav, and Mohit Bansal. Self-chained image-language model for video localization and question answering. *arXiv preprint arXiv:2305.06988*, 2023. [2](#), [4](#), [8](#), [19](#)
- [79] Lu Yuan, Dongdong Chen, Yi-Ling Chen, Noel Codella, Xiyang Dai, Jianfeng Gao, Houdong Hu, Xuedong Huang, Boxin Li, Chunyuan Li, et al. Florence: A new foundation model for computer vision. *arXiv preprint arXiv:2111.11432*, 2021. [2](#)
- [80] Rowan Zellers, Ximing Lu, Jack Hessel, Youngjae Yu, Jae Sung Park, Jize Cao, Ali Farhadi, and Yejin Choi. Merlot: Multimodal neural script knowledge models. *Advances in Neural Information Processing Systems*, 34:23634–23651, 2021. [2](#), [17](#), [18](#)
- [81] Andy Zeng, Maria Attarian, Krzysztof Marcin Choromanski, Adrian Wong, Stefan Welker, Federico Tombari, Aavek Purohit, Michael S Ryoo, Vikas Sindhwani, Johnny Lee, et al. Socratic models: Composing zero-shot multimodal reasoning with language. In *The Eleventh International Conference on Learning Representations*, 2022. [3](#), [8](#)
- [82] Xiaohua Zhai, Alexander Kolesnikov, Neil Houlsby, and Lucas Beyer. Scaling vision transformers. In *Proceedings of the IEEE/CVF Conference on Computer Vision and Pattern Recognition*, pages 12104–12113, 2022. [16](#)
- [83] Bowen Zhang, Xiaojie Jin, Weibo Gong, Kai Xu, Zhao Zhang, Peng Wang, Xiaohui Shen, and Jiashi Feng. Multimodal video adapter for parameter efficient video text retrieval. *arXiv preprint arXiv:2301.07868*, 2023. [4](#)
- [84] Qingru Zhang, Minshuo Chen, Alexander Bukharin, Pengcheng He, Yu Cheng, Weizhu Chen, and Tuo Zhao. Adaptive budget allocation for parameter-efficient fine-tuning. *arXiv preprint arXiv:2303.10512*, 2023. [4](#)
- [85] Zhang Zhang and Dacheng Tao. Slow feature analysis for human action recognition. *IEEE transactions on pattern analysis and machine intelligence*, 34(3):436–450, 2012. [4](#)
- [86] Luowei Zhou, Chenliang Xu, and Jason Corso. Towards automatic learning of procedures from web instructional videos. In *Proceedings of the AAAI Conference on Artificial Intelligence*, 2018. [2](#), [3](#), [4](#)
- [87] Deyao Zhu, Jun Chen, Xiaoqian Shen, Xiang Li, and Mohamed Elhoseiny. Minigt-4: Enhancing vision-language understanding with advanced large language models. *arXiv preprint arXiv:2304.10592*, 2023. [2](#)

A. Methodology Details

Image-to-video architectural adaptations. ViViT with joint space-time attention does not add any new parameters to vanilla ViT, which facilitates transfer between image and video models. However, we change the (position and patch) embedding layers to adapt to video inputs. In particular, we extend position embeddings to longer context via repetition, hence tokens within a frame have the pre-trained position encodings and tokens across time have identical position information. We experimented with both repetition and interpolation for initialization and find that both approaches provide similar results when fine-tuned on video data, whereas repetition works better in a zero-shot setting. As mentioned in Section 3.1 we use 3D convolution for embedding tubelets from the input video. We initialize the convolution weights via the 2D image-based weights by “inflating” them, *i.e.* replicating the filters along the temporal dimension and performing mean pooling [2, 7, 13].

Multi-resolution Patchification and TubeViT. Piergiovanni et al. [52] tune multiple model variants of different sizes on different data mixtures (images vs. videos) in order to achieve good initialization of the multiresolution patch/tubelet embeddings. We aim to avoid additional pre-training steps with multiple pre-trained models and find that initializing all embedding layers with the image-based 2D weights works well in practice. Additionally, Piergiovanni et al. [52] handcraft fixed spatiotemporal position encodings to account for overlapping tubelets with different spatial and/or temporal strides, while showing that learnable position encodings lead to inferior performance. We overcome these obstacles and create a more generic approach that does not need handcrafting by employing factorized attention for processing the different “views” of the video (*i.e.* overlapping parts of the video sampled at different spatiotemporal resolution). We find that this approach leads to better performance in contrast to flatten all multiresolution tubelets and feed them into the joint space-time attention as one long sequence. Following [52], we use four convolution layers with the specified kernels, strides, and offsets. In our exploration, we also try spatiotemporal kernels of (T, H, W) sizes: (4, 16, 16,), (2, 32, 32), and (4, 32, 32).

Adapters and LoRA. We explored use of MLP Adapters [24] and LoRA [25]. For MLP Adapters, we add a bottleneck layer at every layer of the encoder (after the feed-forward block):

$$h_{down,i} = f(LN(W_d h_i + b_d)) \quad (1)$$

$$h_{up,i} = W_u h_{down,i} + b_u \quad (2)$$

$$h_i = h_i + h_{up,i}, \quad (3)$$

where $W_d \in \mathbb{R}^{d_m \times d_b}$, d_m is the model dimension, d_b is the bottleneck dimension (*i.e.* $\ll d_m$), $f(\cdot)$ is a non-linearity (we use *ReLU*) LN is a trainable layer normalization, $W_u \in \mathbb{R}^{d_b \times d_m}$, and h_i is the output of the feed-forward layer.

For LoRA, we decompose the linear QKV input projection, the output self-attention projection, and the dense feed-forward block of each layer in ViViT:

$$h = W_o x + \frac{1}{\alpha} B A x, \quad (4)$$

where W_o is the original weight matrix of each block that remains frozen while tuning the learnable B and A matrices, $B \in \mathbb{R}^{d_m \times r}$, $A \in \mathbb{R}^{r \times d_m}$, $r \ll d_m$ is the rank of the decomposition matrices, and α is a hyperparameter for easier tuning of the model, as recommended by [25].

For ViViT-B experiments: (1) for MLP Adapters, our adapter bottleneck dimension d_b was set to 384 and we zero-initialize weights W_d, W_u and biases b_d, b_u . (2) For LoRA, we use a $r=64$, and $\alpha = 1/64$ and same parameter initialization as [25]. For ViViT-L experiments: the positioning and initialization of adapters were the same as with ViViT-B, but with d_b of 768 (for MLP adapters) and r of 128 (for LoRA).

Temporal pooling + Perceiver resampler. For video-to-text tuning, we use a Perceiver resampler with 3 layers, 1024 model hidden dimension, 8 heads for the multi-head attention blocks and 4096 inner-layer dimension for the feed-forward blocks. The Perceiver resampler was originally introduced by Alayrac et al. [1] in order to produce a fixed number of visual tokens to be fed into the LM independently of the output length of the visual encoder (e.g., for multiple images or videos). However, we empirically find that when we scale to videos beyond 16-32 frames, the Perceiver resampler becomes unstable during training leading to uniform attention distribution over visual tokens, even with appropriate Q/K cross-attention normalization and other tricks. In order to avoid unstable training for long frame sequences, we first average pool visual tokens across the temporal dimension in order to have a fixed number of tokens independently of the video length and then apply Perceiver resampler utilizing the same number of latent queries as the number of input tokens (*i.e.*, 256 in our case for frames of 256x256 spatial resolution and convolution kernel of 16x16 spatial dimensions). Using this combination of a Perceiver resampler and temporal pooling leads to the best performance, compared to alternatives, although performance gains are generally small in comparison to completely removing the Perceiver resampler. We leave to future work the exploration of better ways to project and feed visual tokens into frozen LMs that can scale well with sequence length.

	Image-to-Video Contrastive Pre-training	Short-to-long Video Contrastive Pre-training	Video-to-text Tuning	Dataset-specific Fine-tuning
Optimizer		AdamW		
Learning rate schedule		Cosine with linear warmup		
Gradient clip	2.0		1.0	
Weight decay rate	1e-2		1e-4	
Batch size	512		128	64-128
Base learning rate	5e-5		4e-5	1-5e-6
Linear warmup steps	1k		2k	1k
Training steps	800k	50k	80k	10k
Training steps	800k	50k	80k	10k

Table 4. Training specifications for (1) image-to-video contrastive pre-training, (2) short-to-long video contrastive tuning, (3) video-to-text tuning, and (4) dataset-specific fine-tuning for video captioning.

Training stage	Context	Compute	Duration
Image-to-video contrastive pre-training	Short	64 TPUv3	7 days
Short-to-long video contrastive pre-training	Long	256 TPUv3	1 day
Video-to-text tuning with 400M LM	Short	16 TPUv3	15 hours
Video-to-text tuning with 1B LM	Short	64 TPUv3	2 days
Video-to-text tuning with 400M LM	Long	128 TPUv3	2.5 days

Table 5. Compute resources and duration for training our video-first encoders and video-to-text models used to report results in Tables 2 and 3.

B. Implementation Details

In this section, we discuss implementation details including training specifications, compute resources, synthetic data for training on short and long videos, and evaluation details per benchmark.

Training details. We consider input frames with a 256x256 spatial resolution and patchify videos with a default convolution kernel of 2x16x16. We center-crop all frames and do not consider additional data augmentation or regularization methods. We present our experimental settings categorized by stage of training on Table 4. We report compute requirements for training model variants on Table 5. For offline evaluation, on all tasks and datasets, we used four TPUv5 chips.

Synthetic training data. As mentioned in Section 5, we find that VideoCC3M presents poor video-text alignment and compromises performance of our models. For this reason, we experiment with generating synthetic textual descriptions of the videos via PALI-3 [11]. Videos in VideoCC3M are at 10FPS and on average only 10 seconds

long and static; differences between consecutive frames are small. We roughly sample the center frame from each video and feed it into PALI for generating a detailed description (i.e. selecting the 50th frame, and if this fails, selecting the 25th frame, or if this fails, the 0th frame). We empirically find that (1) generated captions are more accurate than the original, automatically mapped ones, and (2) PALI-3 is able to generate long and detailed captions that mention several details present in the video. We show the effect of adding the PALI-captioned version of VideoCC3M in Appendix C.

Moreover, we use the full-length videos of HowTo100M for training LONGVIVIT on longer contexts (HowTo100M Summary; Section 5). The full-length videos have an average duration of 6.5 minutes and are accompanied by ASR, i.e. automatic closed captions of people describing their actions. However, instead of directly using ASR, which can be noisy, not coherent between utterances, and contains irrelevant information and comments from the speakers, we use a LLM, namely Chinchilla [23], for better cleaning and summarizing the ASR. We further filter generated summaries to discard repetitions. The resulting summaries are more coherent, condensed and describe the desired task and accompanied actions.

Evaluation details per benchmark. For our ablation studies on text-video retrieval (Section 6.1) we use the validation sets of all benchmarks. We follow the settings of Yan et al. [75], when applicable, for reporting our main results in Section 6.2. Specifically:

- *MSR-VTT*: We report results in Table 1 on the full test set for text-video retrieval and on a subset of 1000 examples from the test set for video captioning. Each video is accompanied by 20 different captions, so we report average over the different captions.
- *ActivityNet Captions*: We report results on the `val1` subset. For short video evaluation in Table 2, we consider the first 16 seconds (sampling frames at 1 FPS from the beginning of the video) of the 180-second videos for paragraph-video retrieval and segment-by-segment cap-

	Dataset Size	MSR-VTT		VATEX		YouCook2		ActivityNet	
		T2V	V2T	T2V	V2T	T2V	V2T	T2V	V2T
ALIGN [29]	1B	24.1	17.1	6.2	3.3	1.0	0.5	1.9	1.1
JFT [82]	300M	16.2	14.6	7.6	6.3	1.6	1.0	1.5	<u>3.2</u>
LTIP [1]	324M	27.4	21.0	10.3	5.3	2.7	1.3	3.4	2.4
All Image	1.6B	<u>31.1</u>	<u>27.7</u>	<u>18.6</u>	10.9	3.7	2.4	<u>4.8</u>	<u>3.2</u>
VTP [1]	27M	23.2	21.3	13.3	15.3	2.5	1.9	3.3	3.1
HowTo100M Clips [45]	100M	14.3	13.7	5.6	6.6	<u>9.6</u>	<u>9.9</u>	1.2	1.5
VideoCC3M [47]	7M	12.3	11.9	5.0	4.4	1.0	0.0	1.1	1.0
All Video	134M	26.2	24.7	14.9	<u>15.3</u>	7.7	6.5	4.3	3.0
All	1.8B	<u>36.3</u>	<u>33.8</u>	<u>20.6</u>	<u>23.3</u>	<u>9.3</u>	<u>9.6</u>	<u>6.2</u>	<u>5.1</u>

Table 6. Performance of video model per pre-training image and/or video dataset on zero-shot text-to-video (T2V) and video-to-text (V2T) retrieval (% Recall@1) when trained from scratch. Two best variants are underlined per benchmark.

tions for video captioning. For long video evaluation in Table 3, we consider the raw, full-length videos of `val1` without ground-truth segmentation. There are videos with multiple captions, in which case we report the average.

- *YouCook2*: We report results on the ground-truth segments and full-length videos of the validation set in Tables 2 and 3 respectively.
- *VATEX*: We report results on the validation set for text-video retrieval and on the test set for video captioning. Each video corresponds to 10 different captions, so we report average scores.
- *EgoSchema*: We report results on the released subset with annotations (500 examples in total). We report results for the full set in Section D and discuss limitations. For reporting results on multiple-choice QA, a task that our model has not learned to perform, we follow [44] and InternVideo [65] and train our video-to-text model on MSR-VTT-QA for 5k steps for adapting to the task.

C. Ablation Studies

C.1. Video–Language Pre-training

Here, we provide more insights on video–language pre-training, including data mixtures, model initialization, input context lengths, and auxiliary losses. For our ablations, we use ViT-Base/BERT-medium.

Image and video data mixtures. First, we present performance of our video model (i.e., joint space-time attention) when trained from scratch using different pre-training image and/or video datasets in Table 6. We report Recall@1 for zero-shot text-video retrieval and assess the quality of different pre-training datasets based on downstream performance. Overall, the suitability of each dataset largely depends on the benchmarks. Some key observations in addition to our discussion in Section 6.3 can be summarized as follows:

- Dataset size alone was not a key factor for strong downstream performance (e.g., ALIGN with 1B exam-

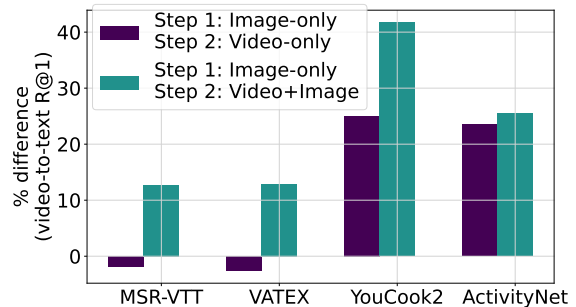


Figure 7. Performance difference (% video-to-text Recall@1) of two step image-then-video training approaches in contrast to training video models on image and video data from scratch.

- Examples (Line 1) vs. LTIP with 324M examples (Line 3) for image datasets, HowTo100M Clips with 100M examples (Line 6) vs. VTP with 27M examples (Line 5) for video).
- Domain match between train and inference time can be a catalyst for good performance, even in cases where vision–text alignment quality is poor (e.g., HowTo100M Clips for YouCook2 (Line 6, third column) in comparison with all other benchmarks). This becomes prominent in video datasets, which tend to be very domain-specific in comparison to image benchmarks.
- Training on videos is important for benchmarks with strong temporal dependencies, but not necessary for benchmarks that largely depend on spatial understanding. In particular, comparing LTIP and VTP which are of similar domain and quality (i.e. collected in a similar way) but of different sizes (324M vs 27M, respectively), we find that MSR-VTT is benefited more by a larger image dataset, whereas video-level information is more crucial than dataset size for VATEX. This further supports our observations from Section 6.3.
- Overall, image and video examples are complementary for video understanding, across all benchmarks.

	MSR-VTT		VATEX		YouCook2		ActivityNet	
	T2V	V2T	T2V	V2T	T2V	V2T	T2V	V2T
Joint ST-ViT (Contrastive only)	39.9	38.1	23.9	26.3	11.4	12.6	6.7	6.4
+ MLM loss	39.0	36.6	23.0	26.4	11.0	12.0	6.8	6.0
+ Captioning loss	39.9	36.0	22.0	24.3	11.2	11.5	6.8	5.6

Table 7. Text-video retrieval results (Recall@1) for different pre-training objectives. We apply 25% masking of the video input in all cases.

Two step image-then-video training. As discussed in Section 3.1, we first train an image ViT-based encoder on images, which we further tune on the video domain via joint space-time attention. This facilitates faster training and stronger contrastive objective due to larger batch sizes (i.e., 8k vs 512). We test the effect of the two-step training approach on zero-shot retrieval in Figure 7. We present % difference on video-to-text Recall@1 when (1) training first on image-only and then video-only, or (2) training first on image-only and then image+video, where the same image datasets are used again with smaller weights for gradient computation, in contrast to jointly train on image+video from scratch. For case (1) we see improvements for two out of four benchmarks. While previous work only continue pretraining on video data [2, 3, 74], we also test keeping image datasets in the pre-training mix (case 2), and surprisingly, we observe an even larger relative improvement across all benchmarks.

Given these observations we conclude that (a) there is indeed a benefit from pre-training first on images and then on videos, but (b) it is important to keep image samples in the mix, since video-text training is noisier and might have negative effect on spatial understanding, which can be mitigated in part from continual training on images. We confirm the latter by also directly evaluating on image benchmarks: for COCOcap [10] an image-trained ViT achieves 35% text-to-video Recall@1, whereas performance drops to 26% for case (1) and 29% for case (2).

Context length. We also experiment with variable number of frames per benchmark at a fixed FPS of 1. We range the number of frames from 2 up to 32 and present incremental performance difference as we gradually increase the number of frames in Figure 8. For most benchmarks, the performance improves as we increase the number of frames up to 16 frames, whereas longer inputs do not show benefits. This result highlights that most current benchmarks do not adequately measure temporal understanding (more than 16 frames). The most challenging dataset is YouCook2, where performance is close to random when considering less than 8 frames. VATEX also presents more challenging temporal dependencies with low performance when considering less than 4 frames. These observations further validate our key findings of Section 6.3 and shed some light on which academic benchmarks are more appropriate to use for eval-

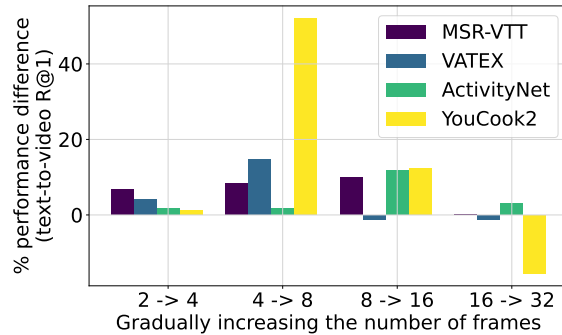


Figure 8. Performance difference (%) for zero-shot text-to-video Recall@1 when gradually increasing the number of frames. This indicates the sensitivity of each benchmark to the number of frames and hence acts as an indicator of the temporal dependencies present in different benchmarks that are widely used.

uating video models.

Auxiliary losses. Although contrastive pre-training is a standard paradigm for image [29, 53] and video training [1, 41, 46, 70], prior work has explored captioning losses for training vision encoders in addition to or instead of contrastive objectives [18, 35, 60, 75, 80]. We next consider variants of the captioning loss for video pre-training as auxiliary losses to the contrastive objective with a 1:1 weighting between the two.

Adding a captioning loss in a dual encoder requires a multimodal encoder/decoder on top for fusing modalities and predicting tokens conditioned on the visual content. We add extra multimodal layers on top of the dual encoder similarly to [75]. We also consider two popular variants of the loss: (1) Masked Language Modeling (MLM), where we consider a multimodal *encoder* and mask 15% of the input textual tokens to predict, and (2) Captioning, where we consider a multimodal *decoder* instead and predict each token of the caption autoregressively. We present results for the different pre-training objectives in Table 7¹⁰. Overall, neither variant is able to improve results; in contrast performance mostly drops by adding the extra objective. Our results contradict prior work’s observations on image pre-training [60] or video pre-training with frozen back-

¹⁰We apply 25% input masking for all variants for more efficient training.

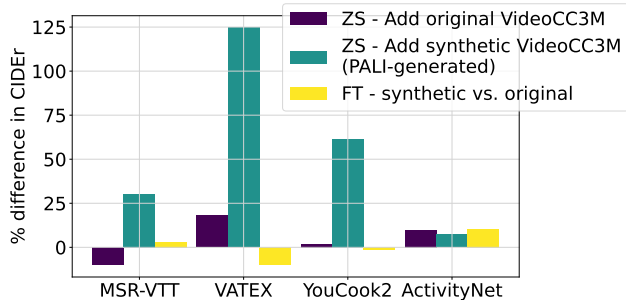


Figure 9. Performance difference (CIDEr) on zero-shot video captioning when we include either the original or synthetic VideoCC3M version (first two bars per benchmark). We also report performance difference between the two variants (i.e., synthetic vs. original dataset) when we fully fine-tune the models (third bar per benchmark).

bones [18, 35, 75, 80] and show that although contrastive objectives might be too coarse-grained for videos, considering captioning losses might be too fine-grained. We hypothesize that the very noisy video-text alignments hurt training of the video encoders when fully fine-tuned and the model needs to predict every textual token, which might not correspond to the visual input. In order to improve video pre-training in future work, we should look at either video-specific training objectives or better video-text alignments for video datasets.

C.2. Video-to-text Tuning

Synthetic VideoCC3M We compare the original and synthetic versions of VideoCC3M (see Section B) for video-to-text tuning in Figure 9. Given a version of SHORTVIVIT-L-to-text tuned only on image datasets from Table 6 and VTP for videos¹¹, we measure % performance difference on CIDEr for zero-shot video captioning when we include either version of VideoCC3M (two first bars per benchmark). We observe a very large performance improvement (up to 125% relative increase) when we use the synthetic version of VideoCC3M for three out of four benchmarks¹². In contrast, using the original version of VideoCC3M provides moderate improvements for two out of four benchmarks (10-20%), no improvement for YouCook2 and has a negative effect on MSR-VTT.

However, observations do not hold when we fine-tune different model versions. In particular, we also report performance difference of the model trained with the synthetic dataset version against the one trained with the original one when we fine-tune them on the target datasets (third column per benchmark). In this case, we do not see benefit by using

¹¹We exclude HowTo100M Clips for short video-to-text tuning, since the dataset is very noisy and leads to drastic drops in performance across most benchmarks.

¹²Improvements for YouCook2 are smaller, i.e. less than 10%.

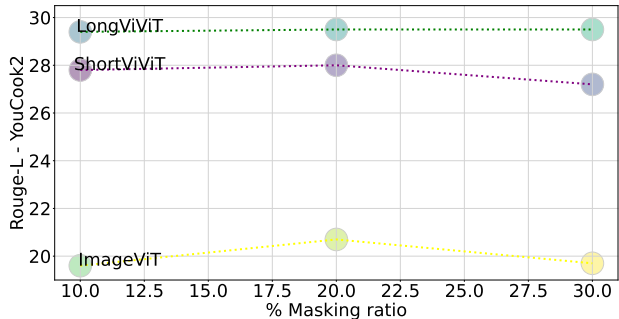


Figure 10. Rouge-L scores for long video models presented in Figure 5 when applying different masking ratios during both training and inference ranging from 10 to 30%.

the synthetic dataset and even suffer performance drop for VATEX (10% relative decrease).

Overall, our findings for using synthetic video datasets are mixed. Our main hypothesis is that synthetic video captions can benefit model training in zero-shot settings since the model learns to produce *longer* and *more descriptive* captions (as empirically observed) which benefits metrics such as CIDEr. However, such benefits vanish when we further tune the model to the domain and style of interest.

Video-to-text Masking We mention in Section 6.1 that we additionally apply up to 30% masking for training and inference on video-to-text. In Figure 10, we present performance (Rouge-L) on video summarization on YouCook2 for the setting described in Section 6.1 when we apply masking at different ratios (10-20-30%) for three model variants: IMAGEViT, SHORTVIVIT, and LONGVIVIT (same models presented in Figure 5). Overall, we do not observe significant performance degradation when considering different masking ratios across all model variants, and hence we used 30% masking for our main experimental results on longer videos (Section 6.2).

D. Additional Experimental Results

EgoSchema full evaluation set. We present our results on both the subset and full set of EgoSchema in Table 8. Overall, we find that blind LLMs can answer a large percentage of questions without requiring any visual grounding (33.2% for the full set in contrast to 27.0% for the subset). Moreover, incorporating visual context to Bard via PALI captioning boosts performance only by 18% for the full set in comparison to 66% relative improvement for the full set. Hence, we find that models utilizing LLMs have an advantage for answering the full set questions and can achieve more competitive performance independently of the quality of the visual encodings. Finally, LONGVIVIT still achieves the best performance for the full set when com-

	ES-Subset	ES-Full
Inference with 256 frames		
IMAGEViT 1B	40.8	30.9
SHORTViViT 1B	47.9	31.0
LONGViViT 1B	56.8	33.3
Modular approaches with 16-frame video models		
SeViLA-to-SHORTViViT	49.6	31.3
IMAGEViT-to-Bard	35.0	35.0
SHORTViViT-to-Bard	42.0	36.2
SeViLA [78] 4B	25.7	22.7
PALI [11] 5B-to-Bard	44.8	39.2
Blind Bard	27.0	33.2
Previous SoTA [44, 65]	–	32.1

Table 8. EgoSchema results (% Accuracy on multiple-choice QA) for subset and full evaluation set.

pared with models employing LMs of equal size, and the original SeViLA [78] model¹³ fails to address the task despite its size (*i.e.* 4B parameters). Given these observations, we overall find the subset to be more challenging than the full set for video understanding evaluation and invite future work to also report performance on the subset for complete comparisons.

Perception Test. We present results on multiple choice video-QA of the recently released benchmark, Perception Test [50]. This benchmark is slightly out of the long video domain – videos are relatively short (<30 seconds), and run at 10 FPS. Nonetheless, we hypothesize that given the nature of questions involving actions and localization, models could benefit from higher FPS and subsequently, longer sequences of input frames. We present results for our model variants and modular methods in Table 9. Indeed, we are able to boost performance when processing videos at 5 FPS considering 256 input frames with LONGViViT (*i.e.* comparison of models in first block of Table 9). Our model still performs better than modular methods that utilize Bard, including PALI-3 for frame captioning. We moreover outperform reported zero-shot results by Flamingo-3B. Finally, we are very close (0.5% absolute difference) to SoTA SeViLA [78], a model with 4B parameters and separately tuned localizer, which however fails to generalize to longer videos and questions about longer-range dependencies (*i.e.* EgoSchema; Table 8).

¹³In the original setting, SeViLA Localizer is trained with 32 input frames uniformly sampled from the video and selects 4 frames to feed to the Answerer.

	PT
IMAGEViT 1B (32 frames @ 1FPS)	39.1
SHORTViViT 1B (32 frames @ 1FPS)	41.9
LONGViViT 1B (256 frames @ 5FPS)	45.7
IMAGEViT-to-Bard	37.8
SHORTViViT 1B-to-Bard	38.8
Flamingo [1] 3B	43.6
SeViLA [78] 4B	46.2
PALI [11] 5B-to-Bard	42.4
Blind Bard	36.8

Table 9. Accuracy (%) on multiple-choice QA on Perception Test (PT). Models in the second and third blocks process videos at 5 FPS, except for Flamingo and SeViLA which follow the settings reported on [50].